

## Analysis of the Inelastic Scattering of Alpha Particles. II†

E. ROST

*University of Pittsburgh, Pittsburgh, Pennsylvania, Oak Ridge National Laboratory, Oak Ridge, Tennessee  
and Palmer Physical Laboratory, Princeton University, Princeton, New Jersey*

(Received July 19, 1962)

The analysis of the inelastic scattering of medium-energy alpha particles is continued using the distorted-waves theory. Attention is given to the qualitative features of these reactions; in particular, the characteristic oscillations in the angular distributions and the associated phase rule. The weak-coupling approximation is studied and is shown to be valid for most medium-energy ( $\alpha, \alpha'$ ) reactions. The distorted-wave theory is compared with alternative theories of inelastic scattering and also with a preliminary sample of experimental data.

### I. INTRODUCTION

IN a previous paper,<sup>1</sup> to be referred to as I, the distorted-wave (DW) theory was developed and specialized to the collective excitation of nuclei by the inelastic scattering of alpha particles. Some aspects of the theory were studied by numerical computation in order to test the sensitivity and reliability of the theory.

In this paper, some of the characteristic results of I will be investigated in more detail and interpreted in simple physical terms. Other theories of the ( $\alpha, \alpha'$ ) reaction will be compared to the DW theory and a preliminary sample of experimental data will be analyzed. A more complete analysis of experimental data will be published later.

### II. QUALITATIVE FEATURES OF ( $\alpha, \alpha'$ ) ANGULAR DISTRIBUTIONS

#### A. $L$ -Space Localization

One of the most striking features of ( $\alpha, \alpha'$ ) reactions is the persistence of sharp, regularly-spaced oscillations in the angular distributions. Such oscillations are a characteristic feature of so-called surface reactions, that is, those involving strongly absorbed particles. In this section, the distorted-waves description of these surface reactions will be analyzed, and illustrated by numerical studies of the  $\text{Ni}^{58}(\alpha, \alpha')\text{Ni}^{58*}$  reactions.

Previous studies<sup>2,3</sup> of alpha-particle scattering have employed the surface approximation for the radial integrals. This approximation assumes a high degree of radial localization in the surface region and may be investigated by introducing an artificial cutoff in the radial integrals which appear in the distorted-waves theory of I,

$$f_{L'L}(R_x) = \frac{k_f}{k_i} \int_{R_x}^{\infty} \chi_{L',(f)}(k_f, r) F_L(r) \chi_{L,(i)}(k_i, r) dr. \quad (1)$$

† This work was supported by the National Science Foundation, the U. S. Atomic Energy Commission, and the Higgins Scientific Trust Fund. This article is based upon the doctoral dissertation of the author at the University of Pittsburgh, 1961.

<sup>1</sup> R. H. Bassel, G. R. Satchler, R. M. Drisko, and E. Rost, preceding paper [Phys. Rev. **128**, 2693 (1962)].

<sup>2</sup> N. K. Glendenning, Phys. Rev. **114**, 1297 (1959).

<sup>3</sup> E. Rost and N. Austern, Phys. Rev. **120**, 1375 (1960). The limitations of the surface approximation are discussed in detail here.

In Fig. 1 we plot the total cross section for the collective excitation of the first excited state of  $\text{Ni}^{58}$  by the inelastic scattering of 43-MeV alpha particles as a function of the lower cutoff radius  $R_x$ . The optical and form-factor parameters are those of the standard set in I. It is clear from the figure that the reaction occurs in the surface region, i.e., between 5.5 and 7.5 F. However, this range is quite large compared to the wavelength of a free alpha particle ( $\lambda=0.37$  F) and one observes a net destructive interference from the smaller values of  $r$ . Thus, the replacement of the radial integrals by the integrands at a "surface" radius would appear to depend quite critically on the value of this radius.

An alternative approach to the understanding of surface reactions makes explicit use of the partial wave expansion and considers a localization of the reaction in angular-momentum space<sup>4</sup> (to be called  $L$  space). The extent of this localization is shown in Fig. 2 where the square of the coefficients  $\alpha_L^m$  of the spherical harmonics (see below) are plotted. The standard DW

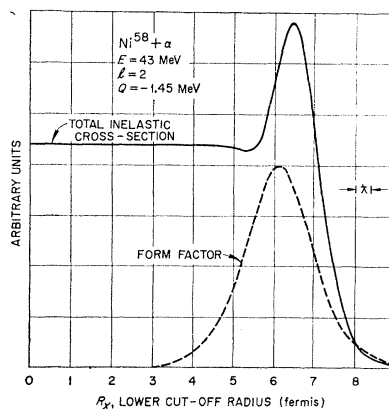


FIG. 1. Total cross section for the inelastic scattering of 43-MeV alpha particles from  $\text{Ni}^{58}$  as a function of the lower cutoff radius  $R_x$  [see Eq. (1)]. The collective-model radial form factor is given by the dashed curve and is the derivative of the optical potential. The optical potential uses a Woods-Saxon shape with parameters  $r_0=1.585$  F,  $a=0.549$  F,  $V=47.6$  MeV, and  $W=13.8$  MeV.

<sup>4</sup> N. Austern, Ann. Phys. (New York) **15**, 299 (1961). See also, N. Austern, in *Proceedings of the International Conference on Nuclear Structure, Kingston, Canada, 1960*, edited by D. A. Bromley and E. Vogt (University of Toronto Press, Toronto, 1960).

case is seen to be dominated by a few partial waves in the vicinity of  $L=18$ . Considerably less localization is found when plane waves are used or when the surface approximation for the radial integrals is employed. The description of the scattering in terms of  $L$ -space quantities is very convenient and will be used repeatedly.

The most important  $L$ -space quantity is the diagonal  $S$ -matrix element,  $\eta_L$ , which determines the elastic scattering, and which is plotted in Fig. 3. One finds very low magnitudes for  $\eta_L$  with  $L < 15$  and a rather sharp transition to  $\eta_L = 1$  over the interval of a few  $L$ .<sup>5</sup> Figure 4 shows this behavior of  $\eta_L$  as a function of energy, and also contrasts it with 40-MeV protons.

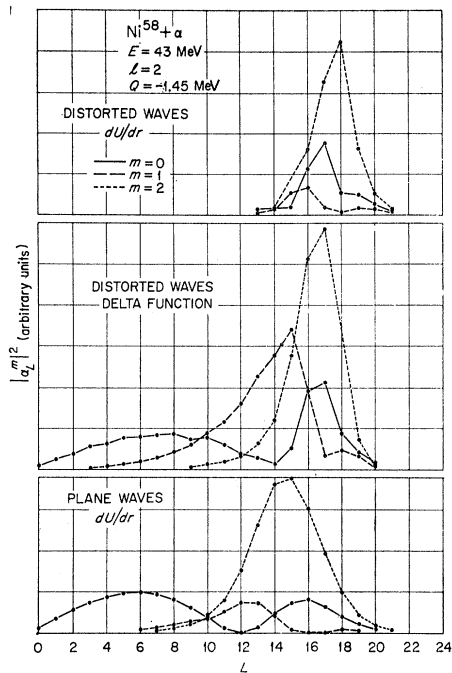


FIG. 2. Study of the relative importance of the spherical harmonics in the inelastic scattering of 43-MeV alpha particles from  $\text{Ni}^{58}$ . The distorted-waves theory of this work is compared to a DW calculation using the surface approximation and to a plane-wave calculation. The  $\alpha_L^m$  coefficients are defined in Eq. (5) of the text.

The latter undergo the transition to  $\eta_L = 1$  at a much smaller value of  $L$  (because of their smaller momentum  $k$ ), and also exhibit much larger fluctuations for small  $L$ . An explanation of the behavior of  $\eta_L$  has been given by Austern<sup>4</sup> in terms of a WKB analysis. In particular, small values of  $\eta_L$  demand a suitable shape of the surface region of the optical potential in order to inhibit reflections. Therefore, it is not surprising to find that the surface thickness,  $a$ , is the most sensitive parameter (see I, Fig. 13).

<sup>5</sup> It is also interesting to note that in the transition region the phase of  $\eta_L$  is roughly constant. This feature lends support to a simple parametrization of the dependence of  $\eta_L$  on  $L$  as is required in a smooth cutoff model.

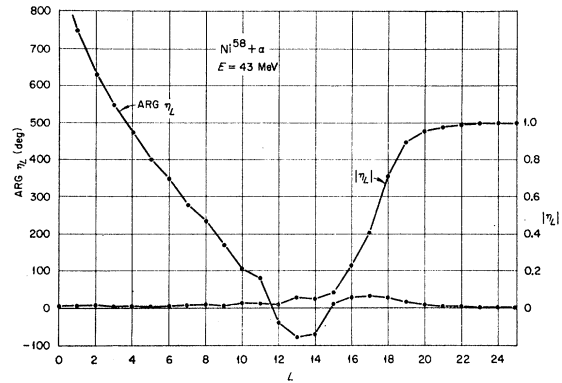
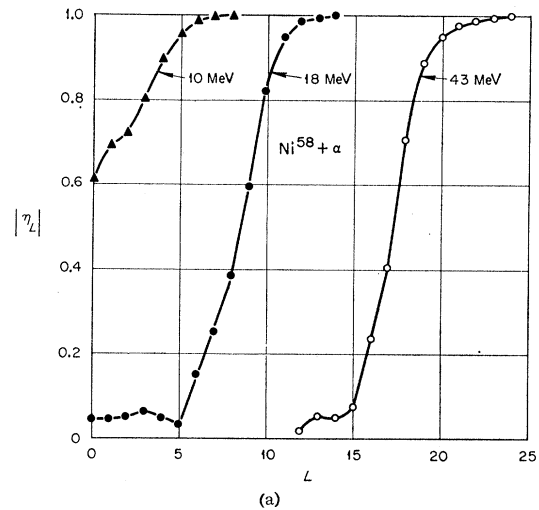
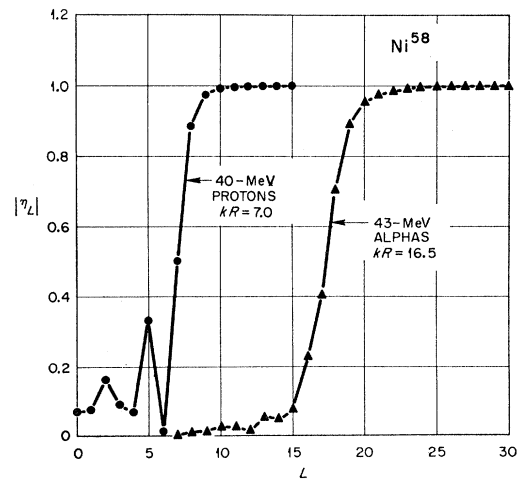


FIG. 3. Diagonal  $S$ -matrix elements  $\eta_L$  for the scattering of 43-MeV alpha particles from  $\text{Ni}^{58}$ .



(a)



(b)

FIG. 4. (a) Study of the variation with bombarding energy of  $|\eta_L|$  for the scattering of alpha particles from  $\text{Ni}^{58}$ . (b) Comparison of  $|\eta_L|$  for 40-MeV alpha particles and 40-MeV protons. All curves were computed using the optical parameters given in the caption to Fig. 1

The "blackness" to the low partial waves contributes to the localization of the inelastic scattering in  $L$ . To see this, we set  $\eta_L=0$  and employ the lowest order WKB approximation which yields<sup>4</sup> for the radial integrals for low  $L, L'$ :

$$f_{L'L} \approx \int dr F_l(r) e^{-i(\kappa_L + \kappa_{L'})r}, \quad (2)$$

where  $\kappa_L$  is the local momentum of the particle as it moves through the combined optical, Coulomb, and centrifugal potential. Since the range where  $F_l(r)$  is appreciable is large compared to  $\kappa_L^{-1}$ , these integrals will tend to average to zero. For those  $L, L'$  corresponding to grazing collisions ( $\eta_L \approx \frac{1}{2}$ ), there is appreciable reflection and the averaging to zero does not occur. This effect is illustrated in Fig. 5 for two typical radial integrals, one with low values of  $L, L'$  and the other with higher values of  $L, L'$ . In this figure we see both the oscillations of the radial integrand [the derivative of  $f_{4,4}(R_x)$  with respect to  $R_x$ ] and the low value of the resulting integral,  $f_{4,4}(R_x=0)$ . The very high partial waves do not contribute because of centrifugal repulsion, i.e., the radial wave functions,  $\chi_L$  are small when  $F_l(r)$  is appreciable and again the integrals tend to zero. The localization is seen to follow from the blackness to the low partial waves and the "size" of the nucleus and has little to do with the detailed nature of the form factor as long as it vanishes rapidly outside

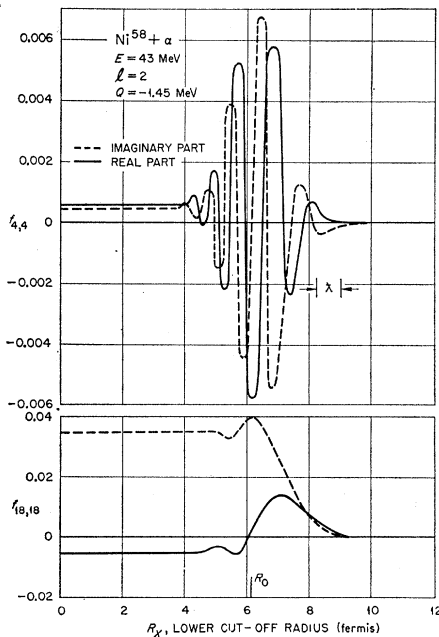


FIG. 5. Radial integrals  $f_{L'L}^{(2)}$  for the inelastic scattering of 43-MeV alpha particles from  $\text{Ni}^{58}$  as a function of the lower cutoff radius  $R_x$ . A typical integral with low values of  $L, L'$  is contrasted with an integral with  $L, L'$  values corresponding to grazing collisions ( $\eta_L \approx \frac{1}{2}$ ) in order to illustrate the phase averaging of the radial integrals for low values of  $L, L'$ .

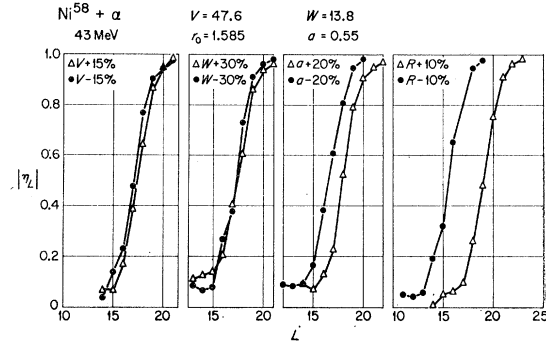


FIG. 6. Effects on  $|\eta_L|$  of varying the parameters  $V, W, R$ , and  $a$  in the DW theory. The effects of these variations on the angular distributions are shown in Figs. 10–13 of I.

the nucleus. Thus, we expect the inelastic angular distribution to be rather insensitive to the form factor and this was amply demonstrated in I.

## B. Effects of Parameter Variations

The localization in  $L$  space suggests that we focus attention on the behavior of a few spherical harmonics. Figure 2 also shows that the terms in the partial wave expansion with  $|m|=l$  are more important than the others. This feature will be studied in detail in the following section. For the present, we assume that the oscillations are characterized by an averaging over a few associated Legendre polynomials. The averaging will be denoted by  $\langle P_L^l(\theta) \rangle_{L_0}$ , where  $L_0$  is an integer near  $kR_e$  and  $R_e$  is some sort of effective nuclear radius. This rough description explains the rapid falloff of the  $(\alpha, \alpha')$  cross section with angle in the forward direction since values of  $P_L^l(\theta)$  for neighboring  $L$  are similar for small values of  $\theta$  but tend to diverge and thus cancel for larger  $\theta$ . For intermediate angles ( $30^\circ < \theta < 150^\circ$ ), one has the asymptotic formula for large  $L$ ,

$$P_L^l(\cos\theta) \approx (-L)^l \left( \frac{2}{L\pi \sin\theta} \right)^{1/2} \times \sin \left[ \left( L + \frac{1}{2} \right) \theta + (2l+1) \frac{\pi}{4} \right], \quad L \gg 1. \quad (3)$$

It is interesting to note that the envelope of the oscillations is given by  $(\sin\theta)^{-1/2}$  which has a minimum at  $\theta=90^\circ$ . Such a minimum has been observed in every distorted wave calculation, although the minimum angle is not always  $90^\circ$ . Another result of the description in terms of Legendre polynomials is that the maxima and minima of the angular distributions should be equally spaced in angle. This feature has been noted in some experiments.<sup>6</sup>

The ideas of  $L$ -space localization are also useful in

<sup>6</sup> L. Seidlitz, E. Bleuler, and D. J. Tendam, Phys. Rev. **110**, 682 (1959).

interpreting the effects of the variation of the parameters in the distorted-wave theory. Figure 6 shows the effect of parameter variations on  $|\eta_L|$  corresponding to the elastic and inelastic angular distributions given in Figs. 10–13 of I. It is readily seen that a 10% change in radius causes a 10% change in  $L_0$  which yields the shifted pattern in Fig. 12 of I. A similar effect occurs when the real optical well depth  $V$  is varied, although the effect is much smaller than when  $R$  is changed. An even more insensitive parameter is the depth of the imaginary potential  $W$ , which seems to have no effect on the spacing of the maxima and minima. The surface parameter  $a$ , however, is a highly sensitive parameter as can be seen in Fig. 13 of I where a modest 20% change in  $a$  causes violent changes in the inelastic (and elastic) scattering. Some of this change is a simple increase in effective radius when  $a$  is increased as shown in Fig. 6. Most of the effect, however, must be attributed to the importance of surface reflections which are highly sensitive to  $a$ . Figure 13 of I dramatizes the importance of the surface shape of the optical potential, the shape being well tested by the elastic and inelastic scattering of medium-energy alpha particles.

Figure 7 illustrates the effects of distortion on the  $\text{Ni}^{58}(\alpha, \alpha')$  cross section. All the curves in the figure were computed using the form factor which gives excellent agreement with experiment (see Figs. 1 and 2 of I). Both the plane-wave case and that computed with Coulomb waves are seen to be in severe disagree-

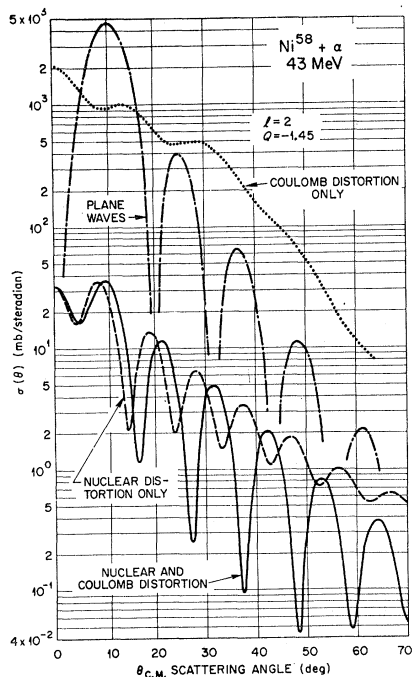


FIG. 7. Effects of distortion on the inelastic scattering of 43-MeV alpha particles from  $\text{Ni}^{58}$ . The collective-model form factor is used with  $\beta=0.18$ .

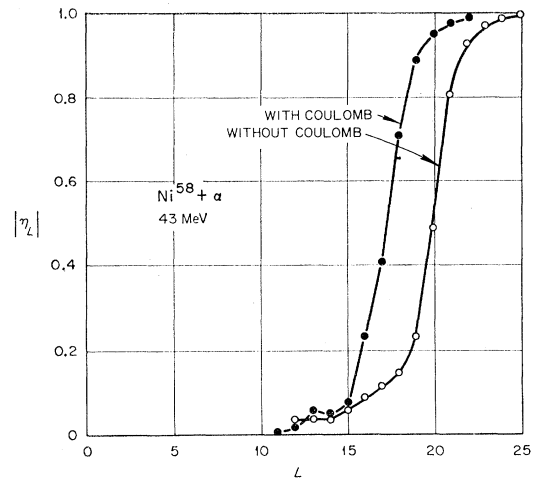


FIG. 8. Effects of distortion on  $|\eta_L|$  corresponding to the angular distributions of Fig. 7. The plane-wave and Coulomb-wave cases of Fig. 7 yield  $|\eta_L|=1$  for all  $L$ .

ment with experiment, especially in their prediction of absolute magnitudes. The nuclear distortion is seen to reduce the cross section to the appropriate magnitude. The primary effect of the Coulomb field is to make the effective nuclear radius  $R_e$ , smaller. A classical formula suggested by Blair<sup>7</sup> interprets  $R_e$  as the impact parameter which leads to grazing collision when the deflection in the Coulomb field is included,

$$R_e = R_0 [1 - (ZZ'e^2/ER_0)]^{1/2}, \quad (4)$$

which yields a 16% decrease in radius for 43-MeV alpha particles on  $\text{Ni}^{58}$ . Figure 8 shows a 12% decrease which is reasonably close to the classical value. It is also interesting to note that the Coulomb field causes a less-damped diffraction pattern which implies a greater degree of localization. This is reasonable, since the slowly varying Coulomb field will reduce surface reflections and thus increase the blackness to the lower partial waves.

### C. The Phase Rule

The adiabatic approximation<sup>8,9</sup> as formulated by Blair<sup>10</sup> predicts a very simple rule relating the angular distributions, resulting from the collective excitation of different levels of a nucleus by inelastic scattering. This rule states that the angular distribution for transitions involving even units of angular momentum transfer are in-phase with each other and out-of-phase with transitions involving odd angular momentum transfer and also the elastic angular distribution. This phase rule has proven to be of considerable value in nuclear spectroscopy.

Since the distorted-wave Born approximation is

<sup>7</sup> J. S. Blair, Phys. Rev. **108**, 827 (1957).

<sup>8</sup> D. M. Chase, Phys. Rev. **104**, 838 (1956).

<sup>9</sup> S. I. Drozdov, Soviet Phys.—JETP **1**, 591 and 588 (1955).

<sup>10</sup> J. S. Blair, Phys. Rev. **115**, 928 (1959).

equivalent to the adiabatic approximation in the limit when both approximations are valid,<sup>3</sup> a phase-rule relationship should also exist here. Furthermore, since the DW treatment is more accurate than the Fraunhofer evaluation of the adiabatic theory, one is able to examine the range of validity of the phase rule.

The formula for the inelastic cross section has been derived in I and may be rewritten as

$$d\sigma_I/d\Omega \propto \sum_m |\sum_L \alpha_L^m Y_L^m(\theta, 0)|^2,$$

$$\alpha_L^m = \left[ \frac{(L+m)!}{(2L+1)(L-m)!} \right]^{1/2} \sum_{\Lambda} \Gamma_{L\Lambda}^{lm} f_{L\Lambda}^l, \quad m \geq 0 \quad (5)$$

$$= (-1)^m \alpha_L^{-m},$$

where

$$\Gamma_{L\Lambda}^{lm} = i^{L-\Lambda-1} (2L+1) \left[ \frac{(L-m)!}{(L+m)!} \right]^{1/2}$$

$$\times \langle L100 | \Lambda 0 \rangle \langle Llm - m | \Lambda 0 \rangle, \quad m \geq 0. \quad (6)$$

The  $\alpha_L^m$  coefficient provides a reasonable measure of the importance of the  $(L, m)$  component in the angular distribution.

Table I presents values of the modulus of  $\alpha_L^m$  for the  $\text{Ni}^{58}(\alpha, \alpha')\text{Ni}^{58*}$  reaction for  $l=2$  and  $l=3$ . The table also includes values of  $|1-\eta_L|$ , which gives an indication of the relative importance of the  $l$ th partial wave in the elastic scattering. Two features are to be noted in Table I: (1) A few high values of  $L$  are much more important than the others; and (2) the largest contributions occur from  $|m|=l$ . The first point has been discussed above and is a result of absorption plus phase averaging of the radial integrals. The second result is new and will be seen to lead to the phase rule.

TABLE I. Values of the  $\alpha_L^m$  coefficients (Eq. 5) for the  $\text{Ni}^{58}(\alpha, \alpha')$  reaction at 43 MeV.

| (a) $l=2, Q=-1.45$ MeV |                    |                    |                    |                    |
|------------------------|--------------------|--------------------|--------------------|--------------------|
| $L$                    | $ \alpha_L^{(0)} $ | $ \alpha_L^{(1)} $ | $ \alpha_L^{(2)} $ | $ 1-\eta_L $       |
| 5                      | 0.0088             | 0.0006             | 0.0013             | 0.989              |
| 10                     | 0.0177             | 0.0025             | 0.0020             | 1.008              |
| 15                     | 0.0438             | 0.0717             | 0.0934             | 0.925              |
| 16                     | 0.1048             | 0.0822             | 0.1259             | 0.803              |
| 17                     | 0.1317             | 0.0436             | 0.1807             | 0.694              |
| 18                     | 0.0717             | 0.0243             | 0.2050             | 0.499              |
| 19                     | 0.0719             | 0.0395             | 0.1261             | 0.264              |
| 20                     | 0.0565             | 0.0351             | 0.0715             | 0.132              |
| 21                     | 0.0308             | 0.0200             | 0.0371             | 0.067              |
| (b) $l=3, Q=-4.5$ MeV  |                    |                    |                    |                    |
| $L$                    | $ \alpha_L^{(0)} $ | $ \alpha_L^{(1)} $ | $ \alpha_L^{(2)} $ | $ \alpha_L^{(3)} $ |
| 5                      | 0.0071             | 0.0021             | 0.0021             | 0.0004             |
| 10                     | 0.0082             | 0.0053             | 0.0033             | 0.0016             |
| 15                     | 0.0882             | 0.0643             | 0.0862             | 0.0810             |
| 16                     | 0.0740             | 0.0667             | 0.0741             | 0.1065             |
| 17                     | 0.0043             | 0.0539             | 0.0576             | 0.1472             |
| 18                     | 0.0197             | 0.0367             | 0.0094             | 0.1097             |
| 19                     | 0.0071             | 0.0237             | 0.0136             | 0.0693             |
| 20                     | 0.0070             | 0.0181             | 0.0122             | 0.0376             |
| 21                     | 0.0082             | 0.0130             | 0.0092             | 0.0201             |

The importance of the  $|m|=l$  quantities is also true for  $l=4$ , but is not presented.

We gain some insight into the reason for the importance of the  $|m|=l$  contribution by examining Eq. (6) in detail. Using algebraic formulas for the Clebsch-Gordan coefficients,<sup>11</sup> it is easy to show that the  $\Gamma_{L\Lambda}^{lm}$  coefficients fluctuate in sign, except for the  $|m|=l$  coefficients which are always positive. Thus, if the phases of the radial integrals,  $f_{L\Lambda}^l$ , are reasonably constant in the interval  $\Lambda-l < L < \Lambda+l$ , the terms in  $\alpha_L^m$  with  $|m| \neq l$  will tend to average out while those with  $|m|=l$  will add. Indeed, examination of the phase of the  $f_{L\Lambda}^l$  integrals for the  $\text{Ni}^{58}(\alpha, \alpha')$  indicates that the phase is quite constant for  $15 < (L, \Lambda) < 20$ , the important region for the inelastic scattering, and explains the dominance of the  $|m|=l$  terms.

The phase of the  $\alpha_L^l$  quantities is also of interest and is given in Table II for  $l=2, 3$ , and 4. One observes that the phase in the "important" region of  $L$  is nearly constant,<sup>12</sup> so that one need only compare the moduli of  $\alpha_L^l$  for different  $l$ . Inspection of Table I shows that these coefficients are large for a few values near  $L=18$

TABLE II. Phase of  $\alpha_L^l$  for different  $l$  for the 43-MeV,  $\text{Ni}^{58}(\alpha, \alpha')$  reaction.

| $L$ | $l=2$  | $l=3$   | $l=4$   |
|-----|--------|---------|---------|
| 5   | 31.0°  | 18.4°   | 18.7°   |
| 10  | -54.9° | -120.5° | -109.8° |
| 15  | 71.7°  | 79.5°   | 70.6°   |
| 16  | 79.8°  | 98.2°   | 82.2°   |
| 17  | 95.5°  | 88.7°   | 104.1°  |
| 18  | 73.4°  | 77.1°   | 72.0°   |
| 19  | 61.2°  | 73.0°   | 64.4°   |
| 20  | 59.7°  | 75.5°   | 64.8°   |
| 21  | 63.7°  | 83.0°   | 69.5°   |

and unimportant for other  $L$ . For forward angles, adjacent Legendre polynomials are very alike. Thus, we would expect similar diffraction patterns from the different cases, if the  $\alpha_L^l$  numbers were coefficients of the same set of Legendre polynomials. However, they are coefficients of associated Legendre polynomials whose  $m$  values differ by one. The angular distributions will therefore obey the phase rule at intermediate angles because of the phase factor  $(2l+1)\pi/4$  appearing in Eq. (3). The  $|m|=l$  requirement may be relaxed a little, the criterion for the DW explanation of the phase rule being that even (odd)  $m$  terms dominate for even (odd)  $l$  and only a small number of partial waves are important. Table I shows that this criterion is well satisfied for the  $\text{Ni}^{58}(\alpha, \alpha')$  reaction.

Another part of the phase rule compares the elastic and inelastic angular distributions. For elastic scattering, one must also consider the low partial waves, since

<sup>11</sup> M. E. Rose, *Elementary Theory of Angular Momentum* (John Wiley & Sons, Inc., New York, 1957), pp. 46, 47.

<sup>12</sup> It is also interesting to note that the phase is largely imaginary as is required for "black" nuclei (see reference 3).

scattering always occurs with absorption. Table I(a) shows that the sharp-cutoff assumption is fairly accurate for the scattering of 43-MeV alphas by  $\text{Ni}^{58}$  with the cutoff at  $L_0 \approx 18$ . Thus the scattering amplitude may be approximated by

$$f(\theta) \propto \sum_{L=0}^{L_0} (2L+1)P_L(\cos\theta) \\ = -\frac{1}{\sin\theta} [P_{L_0}(\cos\theta) + P_{L_0+1}(\cos\theta)], \quad (7)$$

which yields the features of  $l=1$  inelastic-scattering angular distributions. If the inelastic scattering is dominated by  $L \approx L_0$ , then the elastic cross section will be out-of-phase with all even- $l$  transitions. Although the exact value of  $L_0$  is somewhat fuzzy, the phase rule is not much affected, because at forward angles  $P_L^m$  is a slowly varying function of  $L$  but a rapidly varying function of  $m$ .

### III. ALTERNATIVE THEORIES OF $(\alpha, \alpha')$ REACTIONS

#### A. The Adiabatic Theory

An alternative treatment of the inelastic scattering of alpha particles is provided by the adiabatic approximation which has been shown to be equivalent to the distorted-waves method for small collective deformations.<sup>3</sup> The adiabatic method is especially useful for describing the small-angle scattering of particles of small wavelength in which case simple, closed-form expressions are available.<sup>10</sup> For  $l=2$  excitation, for example, one has the equation,

$$d\sigma/d\Omega = [(kR_0)^2/16\pi] \beta_l^2 [J_0^2(kR_0\theta) + 3J_2^2(kR_0\theta)], \quad (8)$$

where  $R_0$  is the surface radius and  $k$  is an average propagation constant  $\hbar^2 k^2/2M = \frac{1}{2}(E_i + E_f)$ . Equation (8) is equivalent to assuming a sharp-cutoff model in partial waves, i.e., the values of  $\eta_L$  are approximated by zero for  $L < L_0$  and by unity for  $L > L_0$ . It should be emphasized that Eq. (8) predicts *absolute* cross sections and has been used to extract values for the deformation parameter  $\beta_l$ . An extension of Eq. (8) to allow for a rounded cutoff in  $L$  has recently been formulated by Blair, Sharp, and Wilets<sup>13</sup> (BSW) who find that the inelastic scattering by quadrupole excitation may be described by a one-parameter family of curves when plotted against  $kR_0\theta$ . The single parameter is (thickness of transition region in  $L$  space  $\div$  critical angular momentum).

Figure 9 shows a graph of the adiabatic and distorted wave theories for the 43-MeV,  $\text{Ni}^{58}(\alpha, \alpha')\text{Ni}^{58*}$  reaction. All curves use the same deformation parameter,  $\beta = 0.18$ . The adiabatic curves assume a surface radius of 6.82 F and the smoothed cutoff curve also uses a smoothing

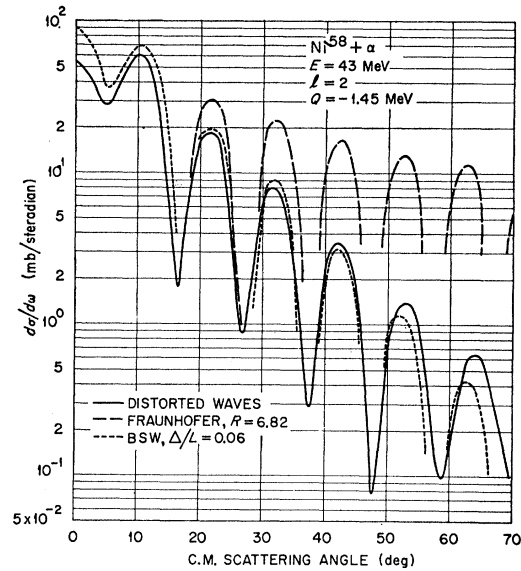


Fig. 9. Comparison of the DW theory with two versions of the adiabatic theory for the inelastic scattering of 43-MeV alpha particles from  $\text{Ni}^{58}$ . The parameters used are described in the text.

parameter  $\Delta/L = 0.060$ . (The latter choice was dictated by the availability of the BSW curves and may be a slight overestimate.) The agreement with experiment<sup>14</sup> is quite impressive, and the location of the maxima and minima are predicted for several orders in the diffraction pattern. The slow falloff for the simple Fraunhofer curve is removed when a rounded cutoff is used. The rounded cutoff model has the advantage of simplicity while the DW method is more general and requires fewer approximations. Both formulations use information from the elastic scattering in order to determine the cutoff or optical parameters and require only a single parameter for normalization of the inelastic scattering.

The curves in Fig. 9 have been normalized with the same deformation parameter  $\beta_l$ . Blair has advocated the employment of the deformation distance,  $\beta_l R_0$ , as the parameter with which to compare different theories.<sup>15</sup> If the midpoint radius of the optical well is assumed to be the appropriate radius, one should multiply the adiabatic curves in Fig. 9 by  $(6.2/6.8)^2 = 0.83$  for comparison purposes. This modification would improve the agreement between the two theories at forward angles although the discrepancy is within the uncertainties of both theories.

#### B. Simplified Distorted-Wave Treatments

The complete distorted-wave calculation which was presented in I is easily performed with a high-speed computer program. However, it is of interest to compare

<sup>14</sup> H. W. Broek, T. H. Braid, J. L. Yntema, and B. Zeidman, Phys. Rev. **126**, 1514 (1962).

<sup>15</sup> J. S. Blair (private communication).

<sup>13</sup> J. S. Blair, D. Sharp, and L. Wilets, Phys. Rev. **125**, 1625 (1962).

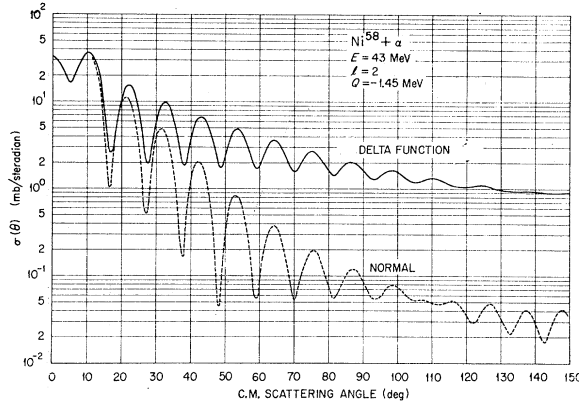


FIG. 10. Comparison of the complete DW theory with one which employs a delta-function form factor  $\delta(r-7.5)$  for the inelastic scattering of 43-MeV alpha particles from  $\text{Ni}^{58}$ . The two curves are normalized at  $0^\circ$ .

these results with those obtained using simplifying calculational assumptions, as in previous DW calculations.<sup>2,3</sup> These simplified treatments may be useful in obtaining a better understanding of the DW theory. It is also possible that an approximate DW calculation will reduce the number of adjustable parameters to the point where universal curves may be generated as in the BSW version of the adiabatic theory.<sup>13</sup>

The primary effort in the complete calculation is the computation of the radial integrals. These integrals have often been obtained by using the surface approximation as discussed in Sec. II(a). In Fig. 10 we compare the angular distributions resulting from this approximation with the complete calculation. The approximation is equivalent to using a delta-function form factor at a radius of 7.5 F; this radius gives the best fit to the angular distribution (the Blair radius in Fig. 9 is 6.8 F). The normalization has been chosen so that the cross section at  $0^\circ$  agrees with the  $0^\circ$  value of the full DW calculation. Qualitative agreement between the curves in Fig. 10 is seen especially in the forward hemisphere for angles greater than about  $20^\circ$ . Since many of the experimental data lie in this region of agreement, the simpler calculation may be of sufficient accuracy, although the normalization procedure is somewhat uncertain. It is interesting to note that an over localization in  $r$  leads to an under localization in  $L$  due to the absence of phase averaging (see Fig. 2) which is seen to cause *more* damping for the sharp-surface angular distributions.

The sharp-surface approximation still requires optical-model parameters in order to generate the distorted waves. A further approximation replaces the exact radial wave functions by their asymptotic form  $\chi_L = \frac{1}{2}ie^{i\sigma_L}[H_L^* - \eta_L H_L]$ , and employs a parametric expression for  $\eta_L$ . For example, the two-parameter expression,

$$\eta_L = \{1 + \exp[(kR_e - L)/\Delta L]\}^{-1} \quad (9)$$

has been found to be useful in the calculation of elastic<sup>16</sup> and inelastic<sup>3</sup> alpha-particle scattering and can be seen from Fig. 3 to be a reasonable approximation for 43-MeV alpha particles on  $\text{Ni}^{58}$ . The use of the asymptotic form for  $\chi_L$  is justified since the radius required in the surface approximation (7.5 F for  $\text{Ni}^{58}$ ) is sufficiently large to be outside most of the optical potential well (see Fig. 1). However, the theory by itself yields only relative ( $\alpha, \alpha'$ ) cross sections and still requires automatic computing facilities.

A sophisticated theory of inelastic scattering which yields absolute cross sections has recently been proposed by Austern and Blair.<sup>17</sup> The essential feature of their theory is the identification of the DW radial integrals with terms proportional to  $\partial\eta_L/\partial L$  (cf. Figs. 2 and 3). The energy difference between initial and final states is ignored. By using simple parametric forms such as in Eq. (9), the computation of the cross section is readily performed. This method may well yield universal curves for medium-energy ( $\alpha, \alpha'$ ) reactions of sufficient accuracy for the extraction of normalization constants from experimental data. However, the theory of Austern and Blair is restricted to rather high energies (because of the adiabatic approximation and the necessity for analytic formulas for  $\eta_L$ ) and, of course, is inapplicable for reactions other than inelastic scattering.

#### IV. PRELIMINARY RESULTS

##### A. Validity of the Distorted-Wave Born Approximation

The total cross section for a given inelastic-scattering reaction which transfers  $l$  units of angular momentum is readily obtained. For an even-even target nucleus, we have

$$\frac{d\sigma_l}{d\Omega} = \frac{k_i(2l+1)}{k_f E_i E_f} A_i^2 \sum_m \sum_{L'L} i^{L'-L-l} (2L'+1)^{1/2} f_{L'L}^l \times \langle L'00 | L0 \rangle \langle L'lm - m | L0 \rangle Y_L^m(\theta, 0)^2. \quad (10)$$

By integrating over angles and using the orthogonality properties of the Clebsch-Gordan coefficients, one arrives at the expression,

$$\sigma_l = \frac{k_i(2l+1)}{k_f E_i E_f} A_i^2 \sum_{L'L} (2L'+1) |\langle L'00 | L0 \rangle f_{L'L}^l|^2. \quad (11)$$

The complete many-channel theory of scattering is expressed in terms of elements of the  $S$ -matrix (or collision matrix) which have as indices the channel, channel spin, and orbital angular momentum. The present problem is simpler, because only two channels are explicitly treated. We will denote an off-diagonal

<sup>16</sup> J. A. McIntyre, K. H. Wang, and L. C. Becker, Phys. Rev. **117**, 1337 (1960).

<sup>17</sup> N. Austern and J. S. Blair (to be published).

$S$ -matrix element by  $\eta_{L'L}(l)$  (the analog in the usual notation<sup>18</sup> is  $S_{\alpha L'l, \alpha 0 L^l}$ ). The integrated cross section for inelastic scattering is written in terms of the  $S$ -matrix elements as

$$\sigma_l = (\pi/k_i^2) \sum_{L', L} (2L+1) |\eta_{L'L}(l)|^2. \quad (12)$$

By equating (11) and (12), one obtains

$$|\eta_{L'L}(l)|^2 = (k_i^3/\pi k_f) [(2l+1)/E_i E_f] \times A^2 |\langle L'00 | L'0 \rangle f_{L'L}^l|^2. \quad (13)$$

The unitarity of the  $S$  matrix demands that

$$|\eta_{L'}|^2 + \sum_L |\eta_{L'L}(l)|^2 < 1, \quad (\text{all } L'), \quad (14)$$

since many other possible channels have been counterfeited by the use of a complex optical potential.

Equation (14) will be investigated for 18- and 43-MeV alpha particles on Ni<sup>58</sup> using a deformation of  $\beta=0.2$  and the standard set of optical parameters. Table III gives values for the absolute squares of the diagonal and off-diagonal  $S$ -matrix elements. As can be seen from the table, the unitarity condition of Eq. (14) is easily satisfied for each partial wave. If  $\beta$  were to become unreasonably large (say, 1 or 2), the statement would no longer be true but this is not important for application to actual nuclei. A similar result was found in the study of other ( $\alpha, \alpha'$ ) reactions at medium energies. The small values for the off-diagonal  $S$ -matrix elements tend to justify the use of "elastic scattering" optical potentials for the DW treatment of inelastic scattering, since these terms reflect the importance of the coupling between the incident and final channel.

We have seen from Table III that the unitarity of the  $S$  matrix is no problem at medium energies. At lower energies this is not necessarily true. The primary reason for the difficulty at low energies is the possible existence of partial wave resonances ( $\eta_L \approx -1$ ). These resonances are often called "shape resonances" and occur when the phase shift passes through  $\pi/2$ . At low energies the projectile wavelength becomes comparable with, or greater than, the (large) surface thickness, and strong surface reflections can occur. These reflections are inhibited at higher energies; in addition, the increased absorption at higher energy yields a much smaller value of  $|\eta_L|$  for low  $L$ . The occurrence of shape resonances at low energies enhances the coupling between the elastic and inelastic channels and makes the distorted-wave Born approximation invalid. The effect of strong coupling may also be important at medium energies for some very light nuclei (e.g., C<sup>12</sup>) and DW calculations for such cases are unreliable.

The distorted-wave Born approximation was criticized by Chase, Willets, and Edmonds<sup>19</sup> who considered

<sup>18</sup> J. M. Blatt and L. C. Biedenharn, *Revs. Modern Phys.* **24**, 258 (1952).

<sup>19</sup> D. M. Chase, L. Willets, and A. R. Edmonds, *Phys. Rev.* **110**, 1080 (1958).

TABLE III.  $S$ -matrix elements for the Ni<sup>58</sup>( $\alpha, \alpha'$ ) reaction.

| (a) 43 MeV                               |              |                       |                       |                       |
|--|--------------|-----------------------|-----------------------|-----------------------|
| $L$                                      | $ \eta_L ^2$ | $ \eta_{L, L-2} ^2$   | $ \eta_{L, L} ^2$     | $ \eta_{L, L+2} ^2$   |
| 8  | 0.019        | $1.1 \times 10^{-4}$  | $6.2 \times 10^{-5}$  | $8.6 \times 10^{-6}$  |
| 10                                       | 0.025        | $5.2 \times 10^{-5}$  | $9.6 \times 10^{-5}$  | $1.1 \times 10^{-4}$  |
| 12                                       | 0.016        | $2.4 \times 10^{-4}$  | $5.8 \times 10^{-4}$  | $3.1 \times 10^{-4}$  |
| 14                                       | 0.049        | $1.06 \times 10^{-3}$ | $9.3 \times 10^{-4}$  | $3.1 \times 10^{-3}$  |
| 16                                       | 0.232        | $2.12 \times 10^{-3}$ | $5.91 \times 10^{-3}$ | $2.02 \times 10^{-2}$ |
| 18                                       | 0.709        | $1.41 \times 10^{-2}$ | $2.13 \times 10^{-3}$ | $6.94 \times 10^{-3}$ |
| 20                                       | 0.956        | $5.27 \times 10^{-3}$ | $1.36 \times 10^{-3}$ | $4.2 \times 10^{-4}$  |
| 22                                       | 0.990        | $3.69 \times 10^{-4}$ | $8.2 \times 10^{-5}$  | $2.7 \times 10^{-4}$  |
| (b) 18 MeV (includes Coulomb excitation) |              |                       |                       |                       |
| $L$                                      | $ \eta_L ^2$ | $ \eta_{L, L-2} ^2$   | $ \eta_{L, L} ^2$     | $ \eta_{L, L+2} ^2$   |
| 4  | 0.047        | $1.23 \times 10^{-4}$ | $9.25 \times 10^{-5}$ | $1.82 \times 10^{-4}$ |
| 6  | 0.157        | $2.66 \times 10^{-4}$ | $2.55 \times 10^{-4}$ | $5.37 \times 10^{-4}$ |
| 8  | 0.392        | $5.47 \times 10^{-4}$ | $5.18 \times 10^{-4}$ | $4.31 \times 10^{-4}$ |
| 10                                       | 0.821        | $3.00 \times 10^{-4}$ | $7.16 \times 10^{-5}$ | $5.5 \times 10^{-5}$  |

the scattering of low-energy neutrons ( $\sim 1$  MeV) by deformed nuclei. Their calculations did not employ the Born approximation and treated the coupling between channels exactly. A marked difference between the DW calculation and the coupled-channels approach was found, especially in the magnitude of the cross section, where the former method was often several times too large. This feature is not surprising at the low energy considered. One, indeed, expects that the effect of the coupling will tend to dampen the inelastic scattering. The amount of damping certainly depends on the strength of the coupling, which may be estimated from the values of the off-diagonal elements obtained by the DW method. The results presented in Table III indicate that the effect is not too important at medium energies. Recent calculations<sup>20</sup> using the coupled channels approach indicate that the DW method is a reasonable approximation for most medium-energy inelastic scattering reactions.

## B. Extraction of $\beta_l$ Values

A comparison of the DW theory to experiment yields a normalization constant which may be identified with

TABLE IV. Summary of ( $\alpha, \alpha'$ ) data.

| Nucleus          | $E_i$ (MeV) | $l$ | $Q$ (MeV) | $\beta_l$            | $\beta_l(\text{EM})^a$ |
|------------------|-------------|-----|-----------|----------------------|------------------------|
| Mg <sup>24</sup> | 43          | 2   | -1.37     | 0.28                 | 0.50-0.66              |
| Ar <sup>40</sup> | 18          | 2   | -1.46     | 0.20                 | 0.16 <sup>b</sup>      |
| Ni <sup>58</sup> | 43          | 2   | -1.33     | 0.18                 | 0.18-0.21              |
| Ni <sup>58</sup> | 43          | 3   | -4.50     | 0.14                 | 0.19                   |
| Ni <sup>58</sup> | 43          | 4   | -5.50     | 0.06                 | 0.14                   |
| Be <sup>9</sup>  | 48          | 2   | -2.43     | 0.5-0.8 <sup>c</sup> | ...                    |

<sup>a</sup> Computed assuming a uniform charge distribution of  $r_0 A^{1/3}$  with  $r_0$  given by electron-scattering experiments. A nonuniform distribution would tend to reduce  $\beta_l(\text{EM})$ , especially for the  $l=3$  and  $l=4$  cases. See A. M. Lane and E. D. Pendelbury, *Nuclear Phys.* **15**, 39 (1960).

<sup>b</sup> Extracted for the 2.4-MeV ( $2^+$ ) state.

<sup>c</sup> Somewhat poorer fits to the Be<sup>9</sup> data have yielded  $\beta_l$  values of 0.5 and 0.6. The application of the simple collective model to such a light nucleus is perhaps questionable.

<sup>20</sup> B. Buck (private communication).



the deformation parameter for collective excitation,  $\beta_l$ , as discussed in I. The same parameter appears in the theory of the excitation of collective levels by electromagnetic means, viz., by  $(e, e')$  reactions, Coulomb excitation, or direct measurements of excited state lifetimes.

A preliminary comparison of the distorted wave and electromagnetic values of  $\beta_l$  is presented in Table IV. The fits for the  $\text{Ni}^{58}$ ,  $\text{Be}^9$ , and  $\text{Ar}^{40}$  cases have been presented in Figs. 2, 7, and 8 of I. A linear plot of the differential cross section for the  $l=2$  and  $l=3$  transitions in  $\text{Ni}^{58}$  is presented in Fig. 11 and emphasizes the excellent agreement between theory and experiment for this nucleus. Figure 12 shows the agreement between theory and experiment<sup>21</sup> for  $\text{Mg}^{24}$  where the optical well has been taken to be the same as that for  $\text{Ni}^{58}$ , except for a small increase in radius. The agreement is seen to be quite satisfactory.

The agreement between the DW theory and electromagnetic values of  $\beta_l$  in Table IV is fair. Blair has suggested<sup>15</sup> that the deformation distance,  $\beta_l R_0$ , is a more appropriate parameter with which to compare normalization constants from different theories. Since

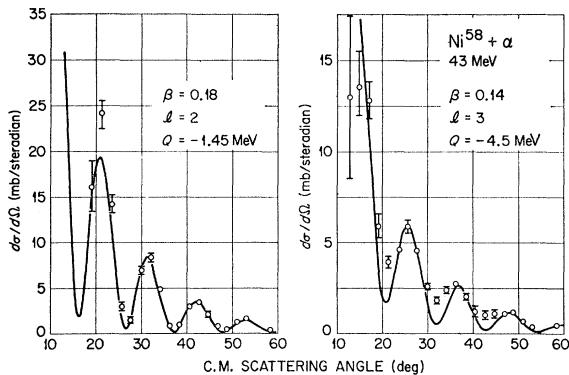


FIG. 11. Differential cross section for the excitation of the  $2^+$  and  $3^-$  states in  $\text{Ni}^{58}$  by the inelastic scattering of 43-MeV alpha particles. The optical parameters are given in the caption to Fig. 1. The experimental points are taken from reference 14.

<sup>21</sup> I. Naqib (private communication). I am indebted to Dr. Naqib for making this data available prior to publication.

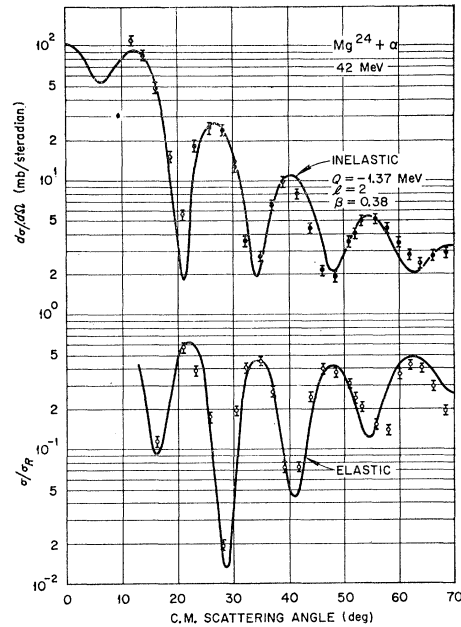


FIG. 12. Preliminary analysis for 42-MeV alpha particles on  $\text{Mg}^{24}$ . The optical parameters are the same as those given in the caption to Fig. 1 except for an increase in radius to  $r_0=1.65$ . The experimental points are taken from reference 21.

the electromagnetic radius is less than the nuclear radius, the adoption of  $\beta_l R_0$  would increase the nuclear normalization relative to the other and definitely improve the agreement for  $\text{Mg}^{24}$ . However, the theoretical and experimental uncertainties are still larger than the disagreement between the  $\beta_l$  values. A detailed analysis of available experimental data is under preparation and should resolve such questions.

#### ACKNOWLEDGMENTS

I would like to express my appreciation to N. Austern and G. R. Satchler for their advice and assistance throughout the course of this work. I am grateful to R. H. Bassel, J. S. Blair, R. M. Drisko, and S. Yoshida for helpful conversations and correspondence. A fellowship from the National Science Foundation is gratefully acknowledged.